consists of crystallites in which stacks of polymer molecules and sheets of water molecules form a non-periodic sequence. A related type of disorder is found in completely different material, *viz.* in random copolymers of two types of monomers that differ in molecular length [5, 6]. Crystallites based on identical but non-periodic sequences within neighbouring copolymer molecules were designated NPL (non-periodic layer) crystallites by Windle *et al.* [6]. Generalizing the concept of NPL crystallites somewhat, the crystallites in partly dehydrated M5 can also be referred to as NPL crystallites. Clearly, the hydrogen bonded water molecules in as-spun M5 contribute to the high fire resistance of the material. The model in Figure 6 suggests that dehydration proceeds via a "zipper" mechanism, so that removal of water molecules from a sheet that has already lost some water molecules has a higher probability than removal of water molecules from an entirely intact sheet of water molecules.

Acknowledgements

This work would have been impossible without the unflagging zeal of Dr Doetze Sikkema in making the M5 project successful. The authors also wish to acknowledge the stimulating interest of Dr. Maurits Northolt and a helpful discussion with Prof. Alan Windle.

References

[1] Sikkema, D.J., *Polymer* (1998) **39**, 5981-5986.

[2] Klop, E.A. and Lammers, M., *Polymer* (1998) **39**, 5987-5998.

[3] Lammers, M., Klop, E.A., Northolt, M.G. and Sikkema, D.J., *Polymer* (1998) **39**, 5999-6005.

[4] "b direction" should be replaced by "a direction" in ref. [2], p. 5996.

[5] Blackwell, J., Biswas, A. and Bonart, C., *Macromolecules* (1985) **18**, 2126-2130.

[6] Windle, A.H., Viney, C., Golombok, R., Donald, A.M. and Mitchell, G.R., *Faraday Disc. Chem. Soc.* (1985) **79**, 55.

X-Ray Analysis of the Network-Forming Collagen in the Dogfish Scyliorhinus Canicula Egg Case

C. Knupp and J.M. Squire

Biological Structure and Function Section, Biomedical Sciences Division, Imperial College School of Medicine, London SW7 2AZ.

Introduction

Network-forming collagens are essential to life for most multicellular organisms. In basal membranes, which are the part of the extracellular matrix that remain in direct contact with their formative cells, they accomplish supportive, protective and filtering roles, and they help cellular attachment, differentiation, migration and growth [1]. In human eyes, the building of abnormal collagen-like networks is related to serious sight threatening diseases that are poorly understood. Of these, age related macular disease alone is responsible for about 50% of the cases of legal blindness in the western world [2]. Structural studies of these molecular organisations are the first step towards understanding their function in the structures that they form or in the pathologies with which they are associated. Unfortunately, in most cases, network-forming collagens assemble into structures that are poorly ordered, making structural investigations particularly difficult. One way round this problem is to find and study in detail a network-forming collagen that assembles naturally in a regular way, in the hope that it can give general insights into the way network-forming collagens behave. The egg case of the dogfish *Scyliorhinus canicula* appears to be a very appropriate candidate for this task. It is formed by a collagen network that naturally possesses a high degree of order. Like the basal membrane it fulfils a supportive, protective and filtering role, being the only medium between the embryo and the sea. Furthermore, its molecular arrangement is strikingly similar to that found in the ocular assemblies associated with age related macular disease.

Dogfish Egg Case

With the naked eye, the capsule containing the dogfish egg appears as a small convex rectangular-shaped container, 50 by 20 mm on average (Figure 1). The two anterior and the two posterior corners are elongated to form horn-like structures that continue their extension as four long, coiled, thread-like

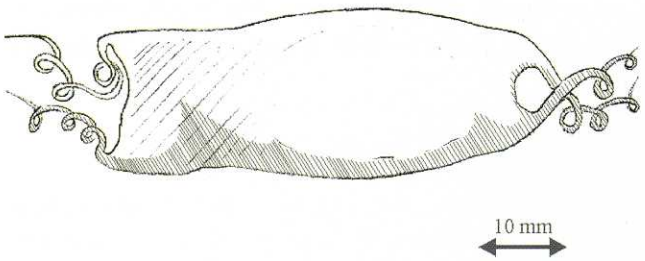

Figure 1: Schematic drawing of the dogfish *Scyliorhinus canicula* egg case. The capsule is about 50 mm x 20 mm and its corners are elongated into four tendrils that attach to seaweeds when the eggs are laid.

filaments, generally referred to as tendrils. These tendrils are used by the females to attach the newly laid eggs to any available supports such as seaweeds or stones. Unlike avian or reptilian egg cases, fish egg cases do not have to prevent water losses, but they still have to allow gaseous exchange for respiration. The dogfish egg case wall has been shown to be highly permeable to small ions and small molecular weight polar solutes, with diffusion channels showing an estimated pore radius of 1.36 nm [3].

Evidence for the collagenous nature of the dogfish egg case [4,5,6] was obtained from X-ray diffraction studies (that indicated the existence of a 0.29 nm meridional arc), thermal shrinkage studies (which produced a thermal shrinkage curve typical for collagen that was S-shaped and with a mean half shrinkage temperature of 78°C) and amino acid analysis (which showed that glycine accounted for about 16% of all amino acid residues with repeated Gly-X-Y regions in the amino acid sequence). The dogfish egg case collagen was purified and observed in the electron microscope after metal shadowing. It appears to be about 40 nm long with a large globular domain at one end (about 4 nm in diameter) and a much smaller one at the other end [7].

The egg case wall is approximately 2 mm thick when wet. It is mainly composed of laminae (about 0.5 µm thick) that become progressively thicker towards the inner surface of the egg case [8,9,7]. In longitudinal sections, the laminae that form the bulk of the thickness of the egg case show a regular alternation of density. Successive laminae show low, intermediate, high, intermediate and low densities and this pattern repeats, more or less regularly through nearly the whole thickness of the egg case. When the laminae are examined at high magnification, the dense ones are seen to contain fibrils sectioned longitudinally, while all the fibrils in the light laminae have been sectioned transversely (Figure 2). The laminae of intermediate density show obliquely sectioned fibrils running parallel to the surface of the egg case. This appearance suggested an orthogonal construction similar to that of plywood in which successive laminae are made up from sheets of parallel fibres [7].

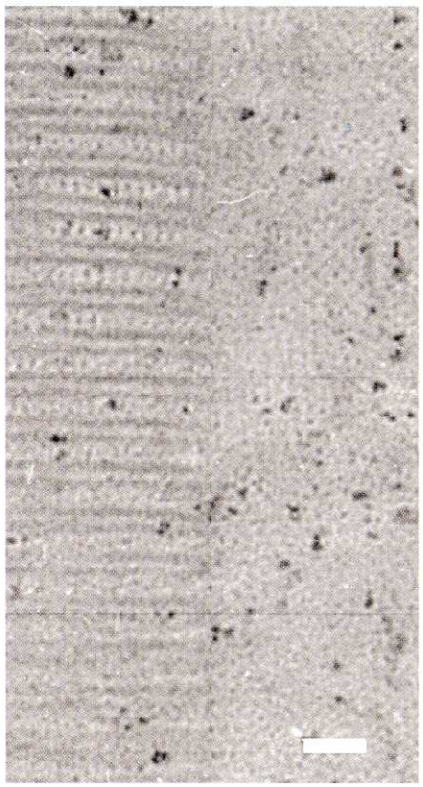

Figure 2: Electron micrograph of the egg case showing two abutting laminae with different fibril orientations. Bar 50 nm.

The fibrils within the laminae appear rather closely packed and show a paracrystalline construction. In transverse section the paracrystalline lattice appears coherent over roughly circular areas up to 150 nm which probably represent the width of the whole fibril. The fibrils present a body-centred square lattice of ordered dots of 10 nm side (Figure 3(a)). In longitudinal sections, pairs of bands of protein density about 13 nm apart can be seen to repeat every 40 nm, with filaments of protein density running axially between the bands (Figure 3(b)). The molecular arrangement within the unit cells was studied using transmission electron microscopy and was found to belong to the *I*422 space group with dimensions of about 10 by 10 by 80 nm [10]. A three-dimensional reconstruction was obtained by combining electron microscope data from different views through the unit cell (Figure 4). A model that fitted the reconstruction was proposed [11] in which

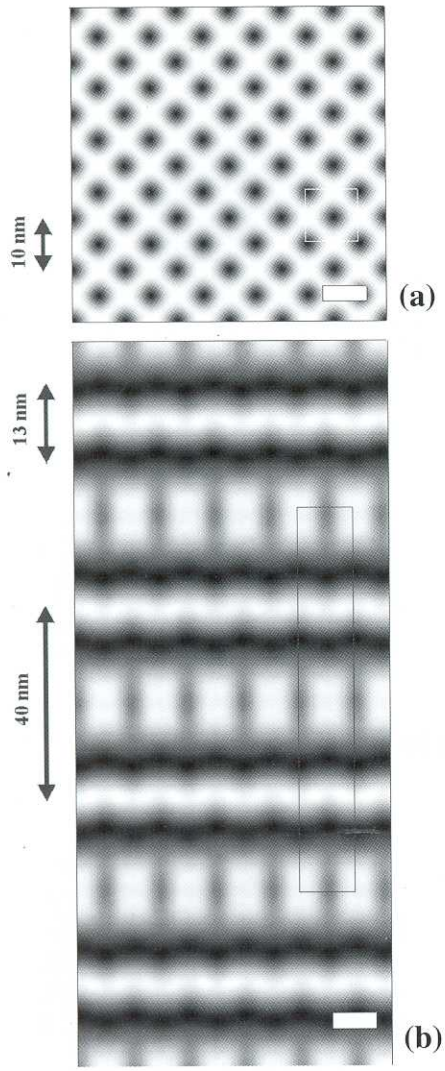

Figure 3: (a) Two-dimensional Fourier synthesis of a transverse appearance of the molecular arrangement in the dogfish egg case. The two-dimensional body-centred unit cell of dimensions about 10 X 10 nm is highlighted in white. (b) Fourier synthesis of a longitudinal appearance. Pairs of bands 13 nm apart are seen running laterally with a 40-nm axial periodicity. Axially, filaments of protein density run through the bands. Proteins are shown in dark tones. Bars 10 nm.

sixteen 40-nm-long collagen molecules occupy each unit cell, with every molecule connected at each terminus to another molecule in a head-to-tail arrangement (Figure 5).

X-Ray Diffraction Studies [12]

Before the X-ray study, pieces of *Scyliorhinus canicula* dogfish egg case wall were removed and washed in distilled water. Successively, laminae were stripped off these and cut into small strips a few hundred microns thick to fit glass capillaries 0.5 mm in diameter. The capillaries were then exposed to the X-ray beam in the beam line 2.1 at the Daresbury synchrotron. The camera was set up with a 2.5 m

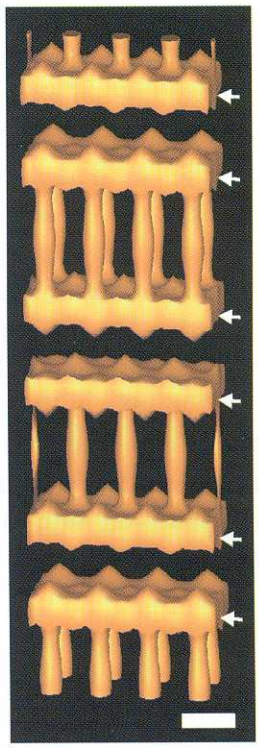

Figure 4: Three-dimensional reconstruction of the molecular arrangement in the fibrils that form the egg case laminae. Arrows highlight the features coming from the lateral pairs of bands seen in Figure 3(b). Axial 'pillars of protein density run between the pairs of bands. Bar 10 nm.

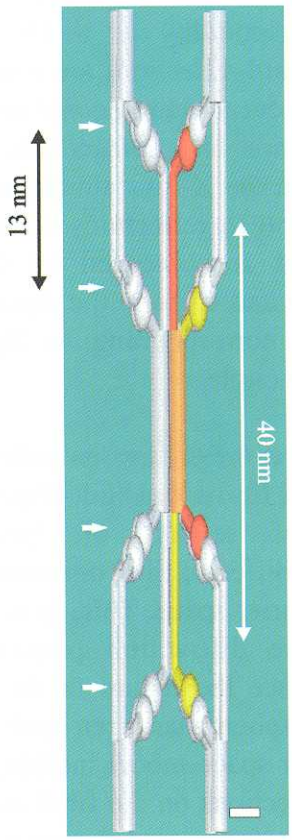

Figure 5: Proposed molecular arrangement within the dogfish egg case unit cell. Sixteen molecules occupy each unit cell. In red and yellow are highlighted two molecules that interact laterally to give rise to the orange filament seen in the figure. Four such filaments associate laterally to give rise to the axial filaments of protein density of Figure 3, or to the axial 'pillars' of the reconstruction in Figure 4. The arrows show the position of the lateral bands (see Figure 3(b) and 4). Bar 3 nm.

long vacuum tube and patterns were collected on an area detector. The acquisition time could vary from a few seconds to 5 minutes. During this time the specimens were kept at 100% humidity by means of a water reservoir in the capillaries. X-ray diffraction patterns of the wall were taken along mutually perpendicular directions, one being perpendicular to the surface of the egg case. Three kinds of diffraction pattern were recorded as shown in Figure 6. One pattern was characteristic of an X-ray direction perpendicular to the laminae in the egg case (Figure 6(a)). Another pattern was observed in either of the two directions parallel to the laminae (Figure 6(b)). A third pattern was observed with the X-rays almost parallel to the plane of the laminae (Figure 6(c)).

The X-ray diffraction pattern obtained with the X-ray beam perpendicular to the laminae (Figure 6(a)), shows rings of intensity corresponding to an 80 nm repeat (arrowheads). In one of the observed patterns with the X-rays parallel to the laminae (Figure 6(b)) even orders of an 80 nm repeat (arrowheads) are present along the meridian. On the equator there is a strong reflection corresponding to a 7 nm spacing (chevron) and on the first layer-line there are two reflections corresponding to a 10 nm spacing (arrows). The 10 nm reflections are connected by an arc which occurs everywhere except on the equator. The 7 nm reflection also smears into arcs. In the pattern taken with the X-rays almost parallel to the laminae (Figure 6(c)), reflections corresponding to an 80 nm repeat are observed on the meridian (arrowheads). On and close to the equator there are three reflections corresponding to 10 nm which prolong to form a circle.

In order to interpret the diffraction pattern, a Fourier space model of the fibrils was built (Figure 7(a)). The superposition of several of these models, corresponding to different fibre directions, gives rise to a model in Fourier space. This, in turn, if correct must explain the diffraction patterns recorded experimentally once the nature of the intersection with the Ewald sphere has been included (Figure 7(b)). The Fourier space model included a series of 80 nm repeat reflections on the fibril axis and rings corresponding to 10 nm and 7 nm spacings. The existence and position of the features included in the model were inferred from the Fourier transform of the electron micrographs of the egg case [10]. Figure 8 illustrates, as an example, the origin of the diffraction pattern in Figure 6(b). Fibres that are 15° apart and with a horizontal 'average' direction (see

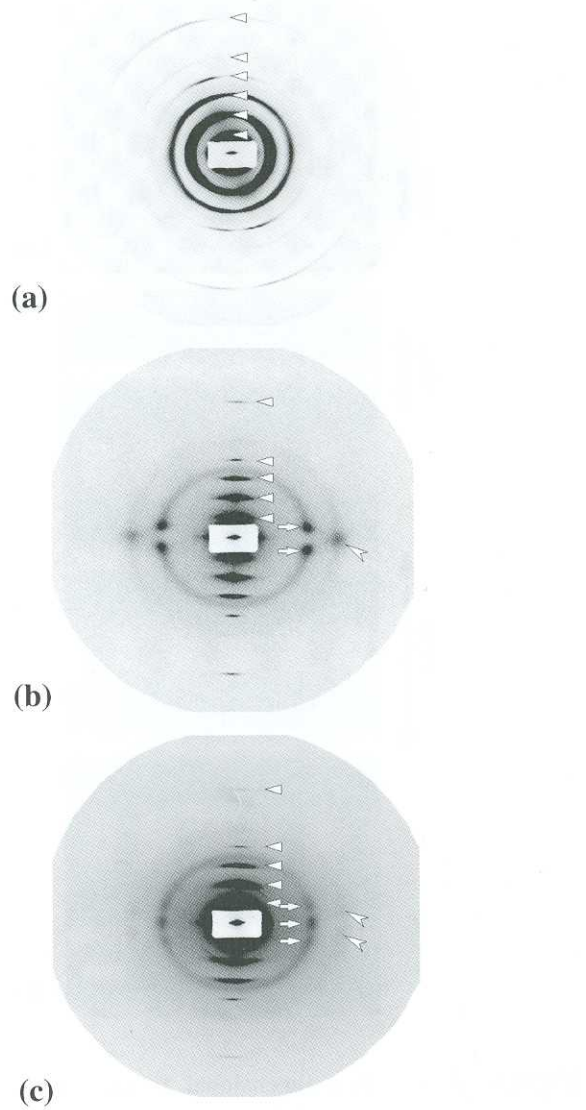

Figure 6: (a) Low- angle diffraction pattern from the dogfish egg case wall obtained with the X-ray beam perpendicular to the laminae in the egg case. Rings of intensity corresponding to orders of a 80 nm repeat are seen (arrowheads). (b) Diffraction pattern with the X-ray beam along a direction parallel to the laminae. On the meridian are even orders of an 80-nm repeat (arrowheads). On the equator there is a strong reflection corresponding to a 7 nm spacing (chevron). The first layer line has reflections corresponding to a 10-nm spacing (arrows). (c) Alternative X-ray diffraction pattern to (b), obtained with the X-ray beam along a direction almost parallel to the laminae in the egg case wall. Reflections corresponding to even orders of an 80-nm repeat are observed on the meridian (arrowheads). On the equator and on a layer-line, it is possible to observe three reflections corresponding to a roughly 10 nm spacing, which lie on a complete circle of intensity. The chevrons highlight two weak reflections corresponding to about 7 nm.

Figure 8(a)) generate the pattern in Figure 8(b) when they intersect the Ewald sphere (a portion of which is drawn in red in Figure 8(a). Fibres oriented vertically (see Figure 8(c)) give the pattern in Figure 8(d). If both main fibre directions are present in the

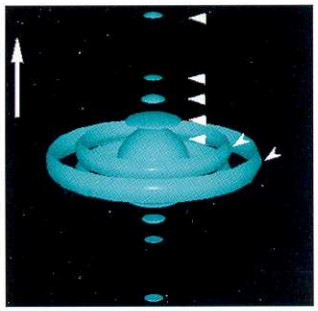

(a)

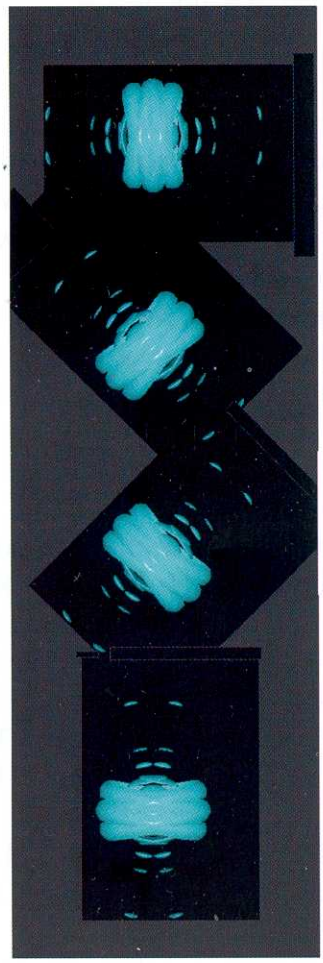

(b)

Figure 7: (a) Model of the Fourier transform associated with the fibres in the egg case laminae. On the fibre axis (directed as the vertical arrow on the top-left side) there are 80 nm repeat reflections, which were inferred from the calculated Fourier transform of the egg-case micrographs. The chevrons indicate rings arising from the meridional and off-meridional reflections, once again inferred from the transforms of the micrographs. These rings are due to random orientation of the fibres around their axes. (b) Models obtained by allowing two main fibril orientations about ± 15° apart along four main directions which are themselves 45° apart. The final Fourier model of the fibrils in the dogfish egg case wall is given by the sum of these models. The meridional rings are omitted for clarity.

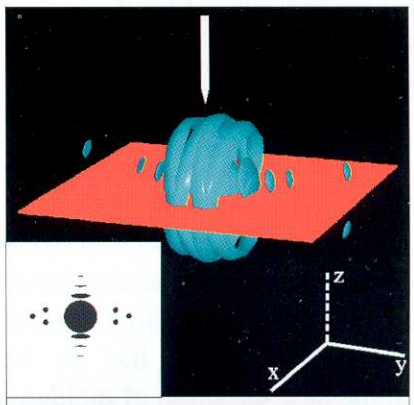

(a)

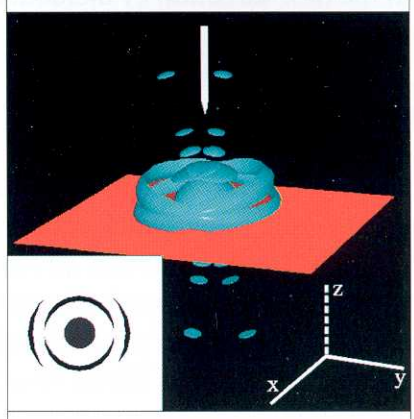

(b)

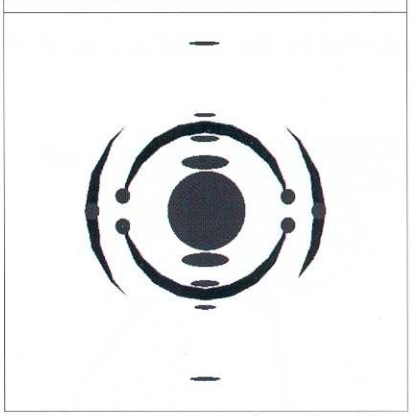

(c)

Figure 8: Origin of the diffraction pattern of Figure 6(b). Fibres which are 15° apart and with horizontal 'average' direction (a) generate the pattern in (b) when they intersect the Ewald sphere (a portion of which is drawn in red in (a)). Fibres oriented vertically (c) give the pattern in (d). If both main fibre directions are present in the specimen, the sum of the two diffraction patterns will be recorded (e). The 10 nm arcs are not prolonged to the equator as they are generated partially by the upper off-meridional reflection ring of the Fourier transform and partially by the lower off-meridional reflection ring (see Figure 7(a)). The gap between the two rings results in the gap between the two 10 nm arcs. Other fibre orientations that lie on the plane generated by the directions of the two fibres previously described are allowed, if the diffraction pattern given by these fibres does not intersect the Ewald sphere except at the 10 nm and 7 nm spot positions.

specimen, the sum of the two diffraction patterns will be recorded (see Figure 8(e)). The 10 nm arcs are not prolonged to the equator as they are generated partially by the upper off-meridional reflection ring of the Fourier transform and partially by the lower off-meridional reflection ring (see Figure 7(a)). The gap between the two rings results in the gap between the two 10 nm arcs. Other fibre orientations that lay on the plane generated by the directions of the two fibres previously described are allowed, if the

diffraction pattern produced by these fibres does not intersect the Ewald sphere except at the 10 nm and 7 nm spot positions.

The other two patterns (Figure 6(a) and (c)) can easily be generated in an analogous way if Fourier space includes the models generated by fibres whose axes lie on planes 45° apart and also have an angular spread around these preferred directions of ±15°. The intersecting Ewald sphere has to be oriented according to the new direction of incidence of the X-rays against the case wall.

Conclusions

The X-ray diffraction patterns can be explained with the hypothesis that the direction of the fibre axes lies in the plane of the laminae and that all the fibres are oriented along a preferred direction within a single lamina. In views down the perpendicular to the laminae, each lamina contains fibrils grouped with a 15° spread of angles around this preferred direction. In views parallel to the laminae, the fibres must be nearly parallel. Successive laminae are arranged with their preferred direction separated by multiples of about 45° (Figure 9). Further, the molecular arrangement seen in the electron microscope is sufficient to explain all of the X-ray diffraction data, suggesting that it is the only one present in any quantity in the egg case wall.

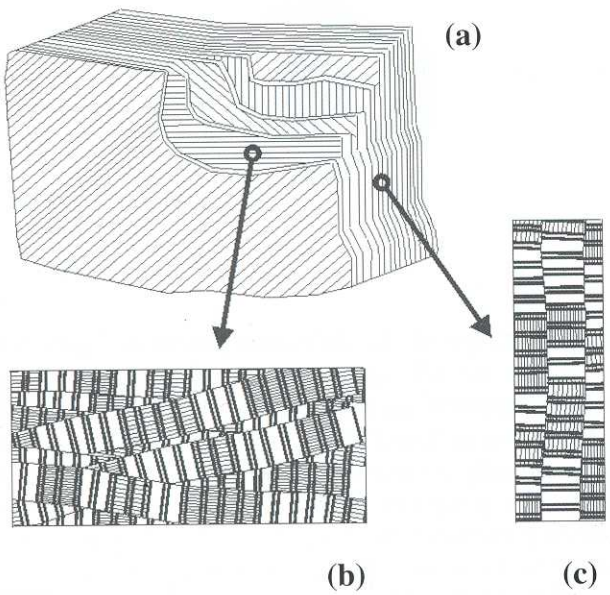

Figure 9: Fibril arrangement in the egg case wall. (a) Portion of the wall showing the changing preferred orientations of the fibrils in successive laminae. Such laminae are about 0.5 μm thick and the orientation change is usually an odd multiple of 45°. (b) Fibril arrangement in a portion of a lamina viewed face-on. The fibrils are about 100 nm in diameter and show preferred orientation with a large spread around this preferred direction of up to ± 15°. Along each fibril, there is only short range order and fibrils show a variable amount of local twisting. Successive pairs of stripes are 40 nm apart. (c) Side view of the arrangement in (b), in which the fibril orientation is almost parallel to the plane of the laminae with only a small degree of orientation.

The egg case wall presumably has many properties in common with the basal lamina in that it has both structural and filtering properties. It may be that the molecular arrangement in the egg case wall will provide insights into the nature of other open network collagens such as type IV, type VI and VIII collagens. It might help to show how type IV collagen influences vital physiological processes such as ultrafiltration in the basal membranes in the kidneys or how the abnormal molecular arrangements in the eyes come to existence.

References

[1] Farquhar, M.G., in *Cell Biology of Extracellular Matrix* (Plenum Press, New York, 1981).

[2] Garner, A., Sarks, S. and Sarks, JP., in *Pathobiology of Ocular Disease* (Marcel Dekker Inc., New York, Basel, Hong Kong, 1994).

[3] Hosney, D., *Experientia* (1978) **34**, 231-40.

[4] Knight, D.P. and Hunt, S., *Nature* (1974) **249**, 379-380.

[5] Rusaouen, M., Pujol, JP., Bocquet, J., Veillard, A. and Borel, JP., *Comp. Biochem. Physiol. B* (1976) **53**, 239-243.

[6] Luong, T.T., Boutillon, M.M., Garrone, R. and Knight, D.P., *Biochemical and Biophysical Research Communication* (1998) **250(3)**, 657-663.

[7] Knight, D.P., Feng, D. and Stewart, M., *Biological review of the Cambridge Philosophical society* (1996) **71(1)**, 81-111.

[8] Feng, D. and Knight, D.P., *Tissue and Cell* (1994) **26**, 155-167.

[9] Feng, D. and Knight, D.P., *Tissue and Cell* (1994) **26**, 385-401.

[10] Knupp, C., Chew, M.W.K., Morris, E.P. and Squire, J.M., *Journal of Structural Biology* (1996) **117**, 209-221.

[11]Knupp, C., Chew, M.W.K. and Squire, J.M., Journal of Structural Biology (1998) **122**, 101-110.

[12] Knupp, C. and Squire, J.M., *Proc. R. Soc. Lond. B.* (1998) **265**, 2177-86.